Obtained results of examination of these areas are indicative of an increased content of oxygen (up to 2.0 %), as well as aluminium (up to 0.4 %) and titanium (up to 0.2 %) compared to their content in the grain body. Apparently, predominant oxidation with formation of Al_2O_3 and TiO_2 oxides runs along the grain boundaries. Presence of oxides along the grain boundaries can promote an increase of stress intensity in these regions, that under certain conditions may lead to fracture propagation through them, which is a possible reason for the obtained results of rupture testing of tubular joints from monel alloy (Table 3).

Results of metallographic investigations are in good agreement with the results of rupture tests. Welds made in two passes have less nonmetallic inclusions and pores compared to single-pass welds and higher strength values, respectively.

Microhardness of the produced joints in the regions of weld metal, HAZ and in the base metal has different values, depending on the material and pass number (Table 4). For the studied materials microhardness after the second pass is more stable, but in the coarse grain section near the fusion line it is somewhat lower than after the first pass.

Investigations of chemical inhomogeneity by X-ray microprobe analysis showed that the uniform and equal distribution of alloying elements in welded joints from steel 304SS, titanium alloy PT-3V and monel alloy is independent on the number of passes.

Thus, orbital EBW process allows producing sound welded joints of tubes from stainless steels, monel alloy and titanium alloys.

1. Masubishi, K. (1989) Space technologies of joints developed in the USA. *Tekhnika Sborki i Soedineniya*, **8**, 103–108.
2. Suezawa, E. (1989) Space stations and colonies. *Ibid*., **9**, 66–75.
3. Paton, B.E., Dudko, D.A., Lapchinsky, V.F. et al. (1973) Application of welding in repair of space objects. *Kosmich. Issled. na Ukraine*, Issue 9, 3–9.
4. Paton, B.E., Lapchinsky, V.F. (1998) *Welding and related technologies in space*. Kiev: Naukova Dumka.
5. Paton, B.E., Lapchinsky, V.F., Stesin, V.V. et al. (1977) Some principles of construction of equipment for technological operations in space. In: *Subject Coll. of 6th Gagarin Readings on Technology in Space*. Moscow.
6. Ternovoj, E.G., Bulatsev, A.R., Solomijchuk, T.G. et al. (2010) Repair of pipelines using orbital TIG welding inside inhabited space objects. *The Paton Welding J*., **4**, 10–13.
7. Paton, B.E. (2000) Space technologies on the threshold of the third millennium. *Ibid*., **4**, 2–4.
8. (2000) *Space: technologies, materials, structures*. Ed. by B.E. Paton. Kiev: PWI.
9. Abramov, E.V., Lyashenko, V.I., Semenov, V.A. (1975) *Automatic welding of steel and titanium thin-wall tubes*: *Advanced methods of treatment of metals and alloys*. Leningrad: LDNTP.
10. (1978) *Welding in machine-building*: Refer. Book. Vol. 1. Ed. by N.A. Olshansky. Moscow: Mashinostroenie.
11. Grinenko, V.I., Belkin, S.A., Astafurova, N.I. (1963) Position butt welding of pipes of steel 1Kh18N9T by self-compression method. *Svarochn. Proizvodstvo*, **10**, 27–29.
12. Roshchin, V.V., Akulov, L.I., Grinenko, V.I. et al. *Self-compression method of welding*. USSR author's cert. 212409. Int. Cl. B 23K 9/16, 37/2. Publ. 05.05.1968.
13. Roshchin, V.V., Uschenko, Yu.S., Bukarov, V.A. et al. (1985) Properties of weld joints made by self-compression method. *IIW Doc. XII-901–85*.
14. Maltsev, M.F., Barsukova, T.A., Borin, F.A. (1960) *Metallography of nonferrous metals and alloys*. Moscow: Metallurgizdat.
15. Bagryansky, K.V., Kuzmin, G.S. (1963) *Welding of nickel and its alloys*. Moscow: Mashgiz.

ELECTRON BEAM WELDING OF HEAT EXCHANGERS WITH SINGLE OR DOUBLE REFRACTION OF THE ELECTRON BEAM

L.A. KRAVCHUK, V.I. ZAGORNIKOV and **I.A. KULESHOV**
E.O. Paton Electric Welding Institute, NASU, Kiev, Ukraine

Selection of energy and time parameters of the electron beam in EBW of tubes to tubesheets of heat exchangers from titanium and the possibility of making a circumferential weld by applying single and double refraction are considered, as well as rotation of the electron beam around the butt using a deflection system. The paper gives the schematic of welding in common vacuum and modes ensuring formation of fillet weld without reducing the pass section of an up to 40 mm diameter tube, including the case when the tubes extend above the tubesheet level.

Keywords: *EBW, electron beam, heat exchanger, tube and tubesheet, welding schematic, single and double refraction, deflecting system, circular and local scan*

At present two fundamentally different technologies of EBW of tubes to tubesheet have become accepted in industry. The difference between them consists in space-time orientation of the electron beam relative to tubesheet plane [1, 2]. In case of single refraction of the electron beam and its rotation around the butt joint by the deflection system relative to a stationary item (Figure 1, *a*) there is a dependence between penetration depth h_{pen}, distance from beam focusing plane to item f_b, tube diameter D_p, and refracted beam deviation in the weld root from tube-to-tubesheet butt Δk:

$$\Delta k = \frac{D_p}{2f_b} h_{pen}.$$

It is seen from this dependence that deviation of refracted electron beam in the weld root from tube-to-tubesheet butt increases with the increase of values

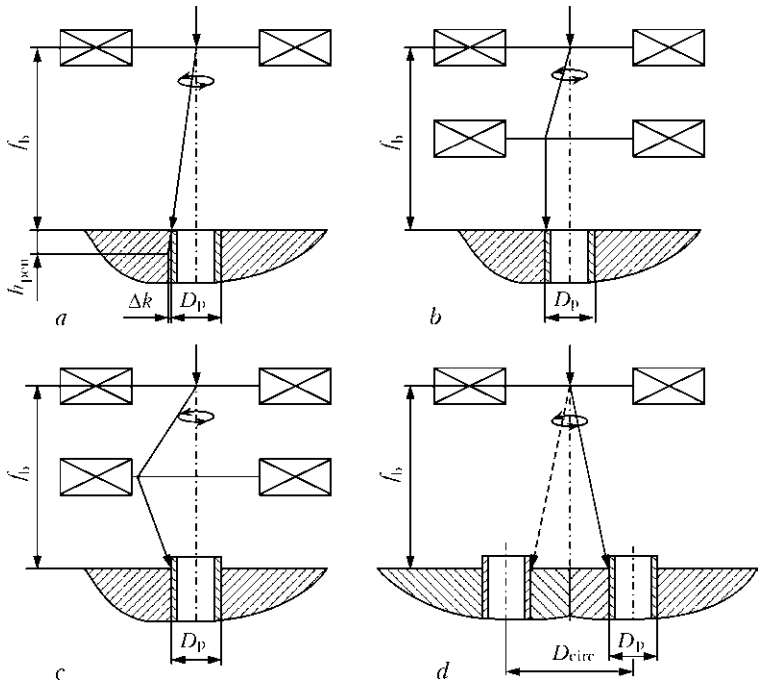

Figure 1. Schematic of EBW of tubes to tubesheets: *a* — single refraction of electron beam and its rotation around the butt; *b* — double refraction of electron beam and its rotation around the butt normal to tubesheet surface; *c* — double refraction of electron beam and its rotation around the butt for tubes extending above tubesheet surface; *d* — electron beam rotation with single refraction and its simultaneous displacement along coordinates x and y along diameter of circumference D_{circ} of shifted tube

D_p and h_{pen} and decreases with increase of f_b. Having selected focal distance f_b = 150 mm and penetration depth h_{pen} = 3.5 mm, we will have the data on the change of weld root deviation from the butt: at D_p = = 8 mm $\Delta k \approx 0.09$ mm, at D_p = 16 mm $\Delta k \approx 0.18$ mm, at D_p = 24 mm $\Delta k \approx 0.28$ mm.

In EBW of tubes with wall thickness δ = 1.0–1.5 mm to tubesheets by the schematic with single refraction of the electron beam (see Figure 1, *a*) in order to ensure $h_{pen}/\delta \geq 2$ ratio, it is necessary to reduce the diameter of beam circular scan d_c by $2\Delta k$ using deflection system, so as to align the weld root with the tube-to-tubesheet butt. This technological measure can lead to flowing of circumferential weld metal inside the tube and reduction of its pass section that is inadmissible in operation of heat exchangers. We believe it is possible to prevent metal flowing inside the tube by application of precision electron beam guns with accelerating voltage U_{acc} = 60 kV and pulsed welding mode [3], as well as limiting tube diameter by $D_p \leq 8$ mm. It should be noted that the precision of electron beam alignment with the circumferential tube–tubesheet butt was not more than 0.05 mm at single refraction and rotation using electromagnetic deflection system.

In EBW of tubes to tubesheets with double refraction of the electron beam and its rotation by the deflection system normal to tubesheet surface (Figure 1, *b*) we believe it is possible to eliminate Δk and prevent flowing of circumferential weld metal inside a tube of diameter $D_p > 8$ mm. The advantage of this technique is protection of anode–cathode accelerating gap of the electron beam gun from breakdowns during welding.

Schematic of EBW of tubes to tubesheets with double refraction of the electron beam and its rotation relative to a stationary product using a deflection system, shown in Figure 1, *c*, allows welding tubes extending above the tubesheet surface. After second refraction the electron beam is guided to the butt of tube and tubesheet at an angle to tubesheet surface, but already with shifting towards it.

Bead deposition on monolithic samples and welding of circumferential tube-to-tubesheet butt joints on PT-7M and PT-3V titanium alloys respectively, were performed in the laboratory unit with electron beam gun ELA-60/15 and Rogowski spherical optics [4], application of which allowed an essential improvement of beam current influence on electron beam focal point position. Two pairs of aligned deflection coils, located coaxially one above the other at 100 mm distance, were used as deflection system. At 63 mm inner diameter of the hole in the coils total height of deflection system was equal to 170 mm (Figure 2).

Control of electron beam focusing on the surface of flat samples and tubesheet at double refraction was checked visually by the brightness of circular scan pattern of diameter d_c = 8 mm with electron beam current I_b = 10 mA on a massive copper plate, located below the tubesheet surface at 2/3 of penetration depth h_{pen}. Such a technique allowed ensuring ratio $h_{pen}/\delta = 4$ without rolls of circumferential weld metal inside the tube on joints of PT-3V alloy tube with wall thickness δ = 1.5 mm to PT-7M alloy tubesheet.

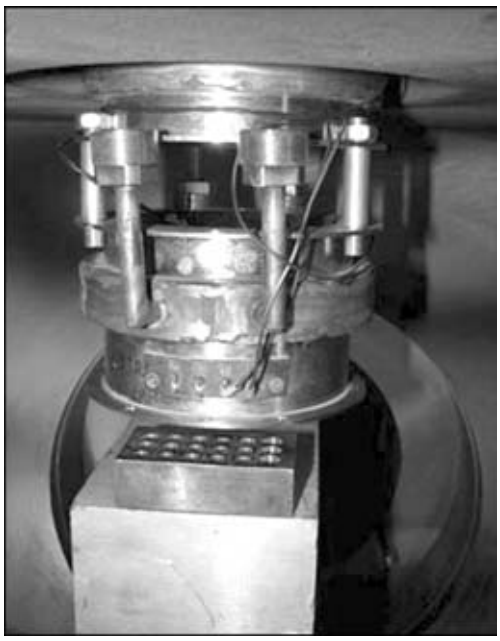

Figure 2. Appearance of deflection system with double refraction of the electron beam mounted on electron beam gun ELA-60/15

To study electron beam heat input and weld face bead width on tube-to-tubesheet welded joints a series of bead-on-plate welds were made by the electron beam with double refraction on monolithic samples from PT-3V titanium alloy at welding speed v_w = = 5–25 mm/s. Penetration depth was kept constant on the level of h_{pen} = 7.5 mm by changing beam current. As shown in Figure 3, heat input q/v_w and weld face bead width B_1 decrease abruptly with increase of welding speed, and starting from v_w = 15 mm/s they are practically stabilized. Minimum weld width reaches B_1 = 1.85 mm. Thus, in further investigations selection of the speed of welding of tube-to-tubesheet joints is performed from the condition $v_w \geq 15$ mm/s. It should be noted that the precision of the electron beam alignment with circumferential butt at double refraction and rotation using two electromagnetic deflection systems was not lower than at single refraction, and was equal to not more than 0.05 mm.

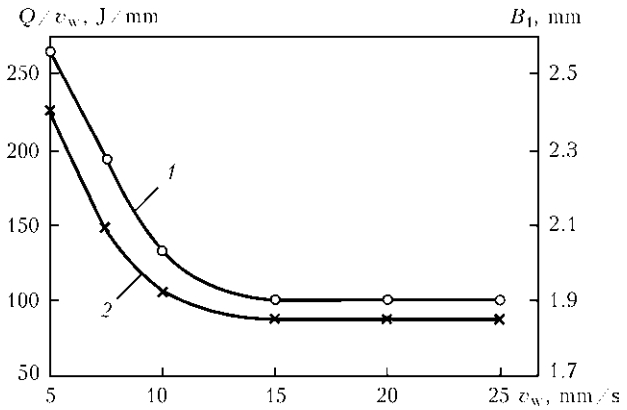

Figure 3. Dependence of heat input q/v_w of electron beam (*1*) and weld face bead width B_1 (*2*) on welding speed v_w in the following welding mode: h_{pen} = 7.5 mm, U_{acc} = 60 kV, I_f = 560 mA, d_c = = 10 mm and f_b = 200 mm

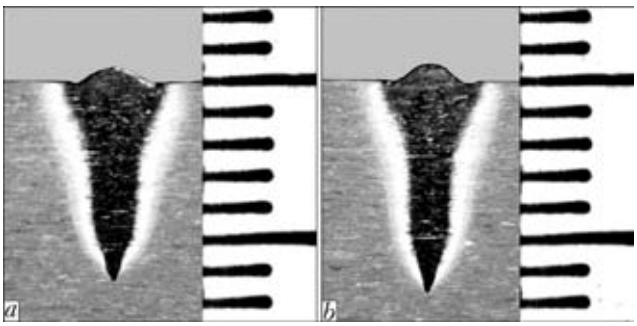

Figure 4. Transverse sections (×7) of beads on titanium alloy PT-3V made by EBW by the electron beam without refraction (d_c = 0 mm) (*a*) and with double refraction (d_c = 40 mm) (*b*) in the following mode: U_{acc} = 60 kV, I_b = 25 mA, v_w = 15 mm/s and f_b = 200 mm

With the schematic of welding with double refraction of the electron beam (see Figure 1, *b*), when after the deflection system the beam is directed normal to tubesheet surface (parallel transfer), the influence of beam double refraction on penetration geometry, and mainly — on penetration depth h_{pen} and weld face bead width B_1 should be studied. To solve this task, a series of bead-on-plate welds were made on a monolithic sample from titanium alloy PT-3V at diameter d_c = 20–40 mm of the electron beam circular scan in tubesheet plane. On transverse sections of the bead (Figure 4) it is seen that geometry of welds (h_{pen}, B_1) made without refraction of electron beam (d_c = 0) and with double refraction (d_c = 40) is practically the same. It leads to the conclusion that the schematic of EBW with double refraction of the electron beam can be recommended for industrial application in welding tubes to tubesheets at up to 40 mm tube diameter inclusive.

In EBW with single and double refraction of the electron beam tube-to-tubesheet welded joints with minimum (about 5 %) fluctuations of penetration depth along the weld length can be made by introducing a circular local scan with the speed not higher than that of welding [5]. Transverse dimensions of weld root part are determined, mainly, by diameter of circular local scan of the electron beam d_{loc}. It should be noted that this technique allows lowering the requirements to the accuracy of alignment of electron beam circular scan, d_c, with the circumferential butt to ±0.15 mm. The series of bead-on-plate welds made on a monolithic sample from titanium alloy PT-3V at variation of diameter of electron beam local scan in the range d_{loc} = 0–1.25 mm with local rotation frequency f_{loc} = 1000 Hz, allowed establishing the change of weld geometrical parameters (h_{pen}, B_1, B_{mid}) and possibility of selection of local scan diameter d_{loc} by width B_1 of weld face bead and width of weld middle part on half the penetration depth B_{mid}. As is shown in Figure 5, at local scan diameter d_{loc} = 0.5 mm welds can be produced with face bead width B_1 = = 2 mm and ratio $h_{pen}/\delta > 3$ at tube wall thickness δ = 1.5 mm. Flowing of circumferential weld metal inside the tube is eliminated.

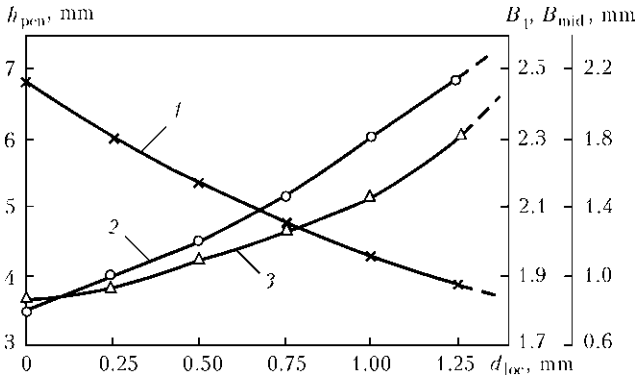

Figure 5. Dependence of penetration depth h_{pen} (*1*), weld face bead width B_1 (*2*) and weld middle part width on mid-depth of penetration B_{mid} (*3*) on diameter of electron beam local scan at U_{acc} = = 60 kV, I_b = 30 mA, v_w = 15 mm/s, I_f = 560 mA, f_b = 200 mm and d_c = 10 mm

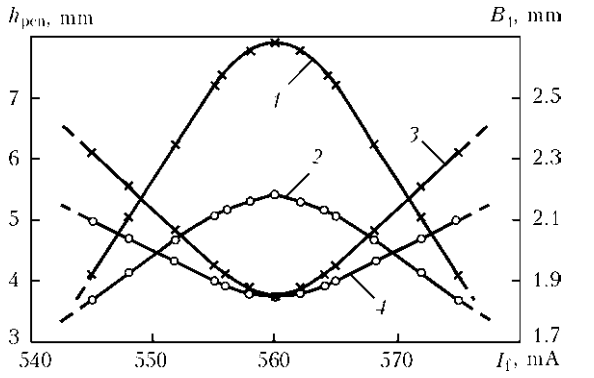

Figure 6. Dependence of penetration depth h_{pen} (*1*, *2*) and weld face bead width B_1 (*3*, *4*) at d_{loc} = 0 (*1*, *3*) and 0.5 mm (*2*, *4*) on focusing lens current I_f at U_{acc} = 60 kV, I_b = 30 mA, v_w = 15 mm/s, f_b = 200 mm and d_c = 10 mm

Influence of electron beam focal point position relative to the surface of tubesheet on penetration depth h_{pen} and width B_1 of weld face bead with double beam refraction was studied by producing a series of bead-on-plate welds on PT-3V titanium alloy at changing of focal lens current I_f from optimum value towards the smaller or greater values by approximately 3 %. Optimum I_f value provides maximum penetration depth h_{pen} and minimum width B_1 of weld face bead. As shown in Figure 6, maximum penetration depth h_{pen} = 7.8 mm corresponds to focusing current I_f = 560 mA and position of electron beam focal point below sample surface on 2/3 of penetration depth. Introduction of circular local scan d_{loc} = 0.5 mm reduces penetration depth by 1.47 times at preservation of face bead width B_1. Change of focusing lens current from optimum value by 0.9 % (ΔI_f = 5 mA) reduces the penetration depth by 0.6 (d_{loc} = 0) and by 0.2 mm (d_{loc} = 0.5 mm). Thus, introduction of a circular local scan of the electron beam allows an essential reduction of the dependence of penetration depth on focusing lens current. In addition, as is seen on transverse sections of the bead-on-plate weld (Figure 7) in EBW of tube-to-tubesheet joints with double refraction of the electron beam and circular local scan an increase of transverse dimensions of the weld middle and root part approximately by value d_{loc} = 0.5 mm is found.

EBW of tube-to-tubesheet joints of heat exchangers can be performed in the case, if a tube of diameter

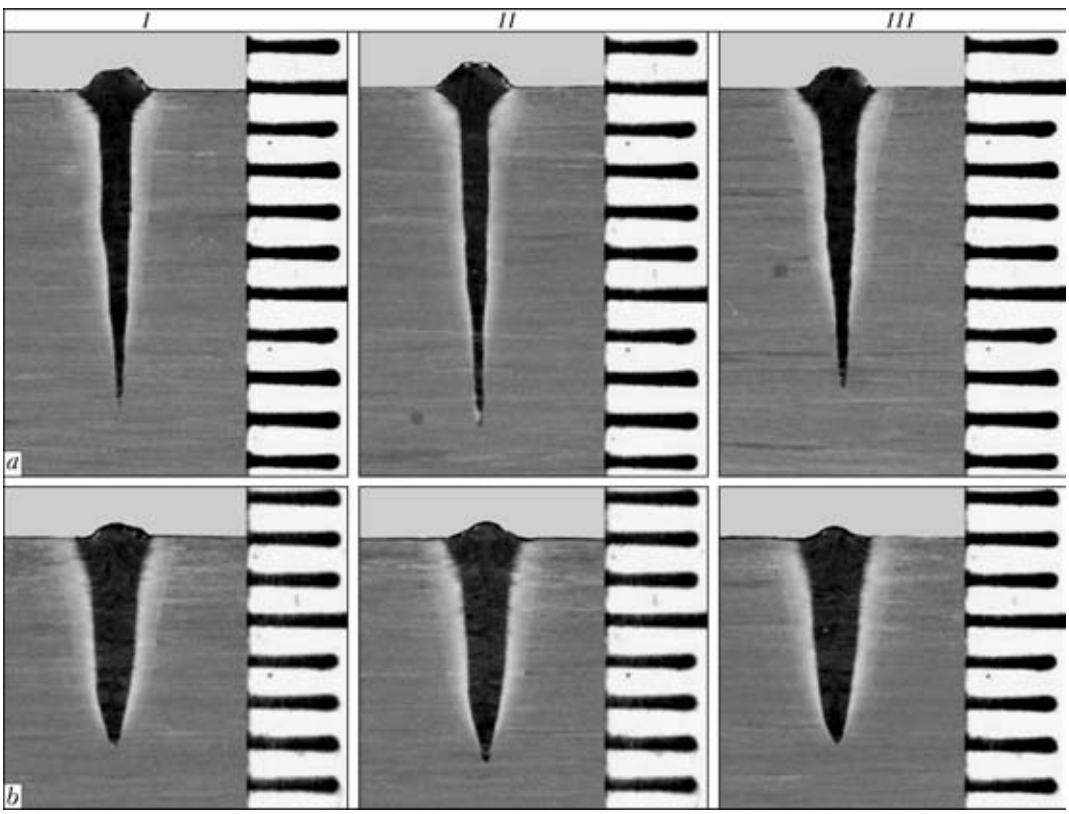

Figure 7. Transverse sections (×5) of bead-on-plate welds on titanium alloy PT-3V made by EBW with double refraction of the electron beam without local scan (d_{loc} = 0) (*a*) and with circular local scan (d_{loc} = 0.5 mm) (*b*) at I_f = 558 (*I*), 560 (*II*) and 562 (*III*) mA in the following mode: U_{acc} = 60 kV, I_b = 30 mA, v_w = 15 mm/s, d_c = 10 mm and f_b = 200 mm

Figure 8. Appearance of specialized system UL-178M for EBW of tubes to tubesheets

$D_p \geq 40$ mm protrudes above the tubesheet surface. To perform this operation the electron beam after the first refraction has to be deflected in such a way that in the refraction plane it would be deployed into a circle of diameter $d_c > D_p$. After second refraction the deflection system directs the beam at an angle to tube axis (see Figure 1, *c*). Weld root alignment with the tube–tubesheet butt is ensured by shifting of the electron beam towards the tubesheet.

In the case, when the tube extends above the tubesheet surface, a welding schematic can be used, at which a tube shifted relative to gun axis for distance $(D_p/2 + \Delta k)$ moves along coordinates x and y by diameter of circumference D_{circ} with simultaneous rotation of the electron beam with single refraction for alignment with the tube–tubesheet butt (see Figure 1, *d*). Such a welding schematic is implemented in specialized system UL-178M (Figure 8) developed at PWI. Two-level multiprocessor automated CNC + + PLC control system allows moving the heat exchanger unit by a certain program inside the chamber along coordinates x and y and controlling the power, focusing and deflection of the electron beam. As shown in Figure 9, in EBW of a tube of diameter $D_p = 27$ mm with 3 mm wall thickness from PT-7M alloy to tubesheet from PT-3V alloy the angle of electron beam deflection from the vertical axis was equal to 4°30′, and its displacement towards the tubesheet was $\Delta k =$ = 0.3 mm for alignment of the weld root with the butt of tube and tubesheet.

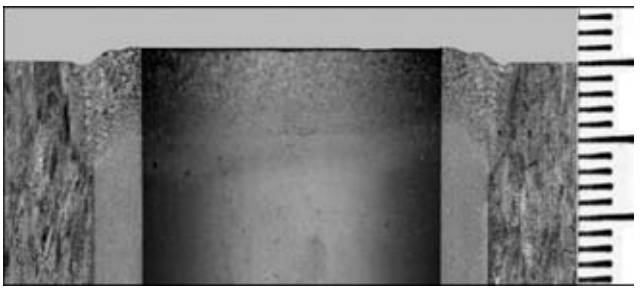

Figure 9. Macrosection (×3) of welded joint of protruding tube ($D_p = 27$ mm with wall thickness $\delta = 3$ mm) with tubesheet produced by electron beam with single refraction and displacement of the tube along coordinates x and y by the diameter of its circumference in the following mode: $U_{acc} = 60$ kV, $I_b = 30$ mA, $v_w = 15$ mm/s and $f_b = 200$ mm

CONCLUSIONS

1. EBW of joints of tube to tubesheet from titanium alloys with double refraction of the electron beam and with rotation around the butt using the deflection system with the stationary workpiece provides formation of the weld without change of penetration geometry up to tube diameter $D_p = 40$ mm inclusive.

2. Minimum values of electron beam heat input and weld face bead width are provided at welding speed $v_w \geq 15$ mm/s.

3. Application of circular local scan of the electron beam at double refraction allows reducing the variation of penetration depth along the weld length, increasing transverse dimensions of its middle and root part and decreasing the dependence of penetration depth on focusing lens current.

4. Double refraction of the electron beam and its rotation around the butt of tube–tubesheet using the deflection system at stationary position of the item allows performing EBW in the case, if the tube protrudes above the tubesheet surface.

5. At such a position of the tube, EBW can be performed by programmed displacement of the tube along coordinates x and y around the circumference with simultaneous rotation of the deflected electron beam around the butt.

1. Goussain, J.C., Penven, Y. (1979) Essais d'application industrielle du soudage par FE pour l'assemblage des tubes sur plaques tubulaires. *Soudage et Techniques Connexes*, 33(**1/2**), 29–42.
2. Trunov, E.N. (1981) Requirements to equipment for electron beam welding of heat-exchange apparatuses. *Avtomatich. Svarka*, **10**, 58–60.
3. Kravchuk, L.A. (1978) Pulsed electron beam welding of tubes to tubesheet of titanium. *Ibid.*, **6**, 53–56.
4. Lawrence, G.S. (1972) Some improvements in beam quality for high voltage beam welders. In: *Proc. of 5th Int. Conf. on Electron and Ion Beam Science and Technology* (Houston, Texas, 1972), 354–371.
5. Kravchuk, L.A., Ugumnov, V.P. (1988) Electron beam welding of thin-walled small diameter tubes to tubesheet. *Avtomatich. Svarka*, **8**, 50–52, 60.